Interaction of Poly(L-Lysine)-*g*-Poly(Ethylene Glycol) with Supported Phospholipid Bilayers

Fernanda F. Rossetti,* Ilya Reviakine,[†] Gábor Csúcs,*[‡] Fabiano Assi,* János Vörös,* and Marcus Textor*

*Bio Interface Group, Laboratory for Surface Science and Technology, Department of Materials, Swiss Federal Institute of Technology, Zurich, Switzerland; [†]Department of Chemical Engineering, University of Houston, Houston, Texas; and [‡]Bio Micro Metrics Group, Department of Mechanical Engineering and Process Technology, Swiss Federal Institute of Technology, Zurich, Switzerland

ABSTRACT   Interactions between the graft copolymer poly(L-lysine)-*g*-poly(ethylene glycol), PLL-*g*-PEG, and two kinds of surface-supported lipidic systems (supported phospholipid bilayers and supported vesicular layers) were investigated by a combination of microscopic and spectroscopic techniques. It was found that the application of the copolymer to zwitterionic or negatively charged supported bilayers in a buffer of low ionic strength led to their decomposition, with the resulting formation of free copolymer–lipid complexes. The same copolymer had no destructive effect on a supported vesicular layer made up of vesicles of identical composition. A comparison between poly(L-lysine), which did not induce decomposition of supported bilayers, and PLL-*g*-PEG copolymers with various amounts of PEG side chains per backbone lysine unit, suggested that steric repulsion between the PEG chains that developed upon adsorption of the polymer to the nearly planar surface of a supported phospholipid bilayer (SPB) was one of the factors responsible for the destruction of the SPBs by the copolymer. Other factors included the ionic strength of the buffer used and the quality of the bilayers, pointing toward the important role defects present in the SPBs play in the decomposition process.

INTRODUCTION

Interactions between lipid membranes and charged macromolecules—such as DNA and proteins—play important roles in many cellular and biotechnological processes. An example of the former is the binding of peripheral proteins to the surface of membranes that can induce lipid demixing, alter phase behavior, and cause other effects (such as alterations in membrane curvature) (Wang et al., 1993; Heimburg and Marsh, 1995; Macdonald et al., 1998; Saurel et al., 1998; Sweitzer and Hinshaw, 1998; Cézanne et al., 1999; Heimburg et al., 1999).

Linear polypeptides composed of basic amino acids (especially polylysines) have been widely used as model systems for the interactions between peripheral proteins and lipid bilayers (Chapman et al., 1974; Hartmann and Galla, 1978; de Kruijff et al., 1985; Carrier and Pézolet, 1986; Laroche et al., 1988; Kim et al., 1991; Kleinschmidt and Marsh, 1997; Diederich et al., 1998; Yaroslavov et al., 1998; Huster et al., 2000; Sagristá et al., 2000; Franzin and Macdonald, 2001; Yaroslavov et al., 2003). They were found to induce domain and pore formation, enhance the flip-flop rates of lipid molecules, alter the phase behavior of the lipids, influence bilayer stability, etc. These systems are also useful for distinguishing the effects of membrane insertion (occurring for proteins with hydrophobic domains) from electrostatically mediated adsorption.

On the biotechnological side, examples of important processes include DNA-phospholipid interactions (relevant for gene delivery studies) that have lead to the discovery of novel soft biomaterials (Golubovic and Golubovic, 1998; O'Hern and Lubensky, 1998; Pfohl et al., 2002), the formation of supported bilayers on polyelectrolyte-coated surfaces (Sackmann and Tanaka, 2000) and the coating of liposomes with various polyelectrolytes with the aim of stabilizing them (Laroche et al., 1988; Sagristá et al., 2000; Kawakami et al., 2001; Ge et al., 2003) or tailoring the release of their contents in drug delivery applications (Kozlova et al., 2001). The issue of stability is a crucial one for the use of lipidic systems in biosensor technology (Terrettaz et al., 2003).

The studies cited above have essentially focused on polyelectrolytes of simple structure: homopolymers (linear or branched) or random copolymers. Because quite a few membrane-binding proteins are either modified hydrophobically (e.g., myristoylated; see Alberts et al., 1994) or form membrane-inserting domains (Kuhn et al., 2002; Epand, 2003; Peisajovich and Shai, 2003), significant research efforts have also focused on polymers bearing hydrophobic moieties (Ringsdorf et al., 1993; Lipowsky, 1995; Ladavière et al., 2002). To the best of our knowledge, research regarding the interactions between block copolymers or graft copolymers containing only hydrophilic moieties has been limited (Bronich et al., 2000). In this study, we investigate the interactions of poly(L-lysine)-*graft*-poly(ethylene glycol) (PLL-*g*-PEG; Sawhney and Hubbell, 1992; Elbert and Hubbell, 1998) with supported phospholipid bilayers (SPBs; see Watts et al., 1984; Sackmann, 1996) and supported vesicular layers (SVLs; Nollert et al., 1995). This polymer was chosen for the favorable properties it imparts to the negatively charged surfaces it adsorbs to: resistance to

nonspecific protein adsorption (resulting from the densely packed PEG chains; see Kenausis et al., 2000; Huang et al., 2001; Ruiz-Taylor et al., 2001a,b; Pasche et al., 2003) and the ease with which functional groups can be included in its structure (Ruiz-Taylor et al., 2001a; Huang et al., 2002; Csúcs et al., 2003; VandeVondele et al., 2003). The extensive hydration of the PEG side chains may furthermore enhance the stability of the coated lipidic bilayers against drying and destruction by chemical and biological agents. ''Stealth'' liposomes, containing PEG-bearing lipids, are well known for their ability to evade the body's defense systems (Woodle and Lasic, 1992), but a generic polymer coating offers more versatility, in that it can be used to modify any negatively charged lipidic or polymeric vesicles.

MATERIALS AND METHODS

Materials

The phospholipids used in this study—dioleoyl phosphatidyl choline (DOPC), dioleoyl phosphatidyl serine (DOPS), and fluorescently labeled nitrobenzoxadiazole-phosphatidyl choline (NBD-PC)—were purchased from Avanti Polar Lipids (Alabaster, AL). Fluorescently labeled tetramethylrhodaminethiocarbamoyl phosphatidyl ethanolamine (TRITC-PE) was obtained from Molecular Probes (Leiden, The Netherlands). Poly(L-lysine)-*graft*-poly(ethylene glycol) (PLL-*g*-PEG), was synthesized in house from poly(L-lysine) hydrobromide (PLL, 20 kDa, Sigma, Buchs, Switzerland) and an *n*-hydroxysuccinimidyl ester of methoxy-terminated poly(ethylene glycol) (mPEG-NHS, 2 kDa, Shearwater, Huntsville, AL) according to a procedure published previously (Kenausis et al., 2000; Huang et al., 2001). The grafting ratio (the number of lysine units per PEG side chain) was determined by proton NMR in D_2O on a 300-MHz spectrometer to be ~ 2.9 (Huang et al., 2002). Fluorescently labeled PLL-*g*-PEG was synthesized in-house according to a previously published protocol (Csúcs et al., 2003), using a PLL (20 kDa) backbone and both PEG (2 kDa) and PEG-fluorescein (5 kDa) side chains. The grafting ratio, as determined by proton NMR in D_2O, was ~ 4.0, and the percentage of fluorescein-terminated PEG chains relative to the total number of PEG-containing side chains was found to be 25%.

Poly(ethylene glycol) (PEG, 2 kDa, Fluka, Buchs, Switzerland), PLL, and PLL(20 kDa)-[$g = 14.2$]-PEG(1 kDa) (Pasche et al., 2003) were used in control experiments.

Chloroform was purchased from J.T. Baker (Phillipsburg, NJ) and sodium dodecyl sulfate from Sigma.

Three different buffers were used throughout this study: H1 buffer, containing 10 mM HEPES (Fluka); Ca^{2+} buffer, containing 10 mM HEPES, 100 mM NaCl (Fluka) and 2 mM $CaCl_2$ (Sigma); and EDTA buffer, which contained 10 mM HEPES, 100 mM NaCl, 2 mM EDTA (Sigma). In all cases the pH was adjusted to 7.4 with a 6 M solution of NaOH.

Water used throughout the study was from a Milli-Q Gradient A10 (Millipore, Volketswil, Switzerland).

METHODS

Vesicle preparation

Multilamellar vesicles were prepared by mixing appropriate amounts of lipids dissolved in chloroform and evaporating the solvent with argon. After at least 30 min of drying in a vacuum oven (Bioblock 45001, Fisher Bioblock Scientific, Illkirch, France) connected to an oil-free diaphragm vacuum pump (Model MZ2D, Vacuubrand, Wertheim, Germany), the lipids were resuspended by vortexing in the Ca^{2+} buffer at the desired concentration. Unilamellar vesicles were obtained by extruding multilamellar vesicle suspensions through polycarbonate membranes with pores of appropriate diameter (Avestin, Ottawa, Canada) using a Lipofast extruder (Avestin).

Substrate preparation and cleaning

Silica-coated quartz crystals for use in the quartz crystal microbalance with dissipation (QCM-D, Rodahl et al., 1995) experiments were purchased from Q-Sense AB (Gothenburg, Sweden). For fluorescence microscopy studies, round glass coverslips (Menzel Gläser, Braunschweig, Germany) were coated with 12 nm of SiO_2 on top of a 12-nm-thick layer of TiO_2 by reactive sputtering in a Leybold DC-magnetron Z600 sputtering unit at the Paul Scherrer Institut (PSI, Villigen, Switzerland) as described previously (Kurrat et al., 1997). Both kinds of substrates were cleaned in a 2% sodium dodecyl sulfate solution for at least 30 min, rinsed with ultrapure water, and treated in a preheated UV/ozone cleaner (Model 135500, Boekel Industries, Feasterville, PA) for 30 min.

Quartz crystal microbalance with dissipation (QCM-D)

Quartz crystal microbalance with dissipation (QCM-D; Rodahl et al., 1995) measurements were performed with a QAFC301 axial-flow chamber attached to a QE301 electronics unit (Q-Sense AB). Immediately after cleaning, a crystal was mounted in the flow chamber of the instrument and checked for resonance on the fundamental (~ 5 MHz) and overtones ($\sim 3\times$, $5\times$, and $7\times$ the fundamental frequency). If all four resonance frequencies could be found, the chamber was filled with the Ca^{2+} buffer, and the four sets of resonance frequencies and dissipation factors were recorded continuously. Once the drift in the resonance frequencies and dissipation factors had settled out, they were recorded for a further 10–20 min (to acquire a baseline), after which 0.5 ml of temperature-equilibrated suspension of unilamellar vesicles at 0.5 mg/ml lipid concentration was injected into the measurement chamber. Temperature equilibration was achieved by letting 1.5 ml of solution flow through the instrument's T-loop and allowing it to equilibrate there for 3 min before the injection into the measurement chamber. Bilayer formation occurred spontaneously upon injection of vesicles into the chamber (Fig. 1) and was allowed to proceed to completion, as judged by the return of the dissipation value to the baseline level (Keller and Kasemo, 1998). Excess of vesicles was removed by rinsing the measurement chamber with 0.5 ml of temperature-equilibrated Ca^{2+} buffer.

Polymer-bilayer interactions were investigated by injecting 0.5 ml of 0.5 mg/ml temperature-equilibrated solutions of PLL-*g*-PEG, PLL, or PEG in an appropriate buffer into the measurement chamber. Before injecting the polymer, the SPB was rinsed several times with the buffer in which the polymer was dissolved (until no further frequency/dissipation factor changes could be observed upon rinsing). Stability of SPBs to buffer exchanges was
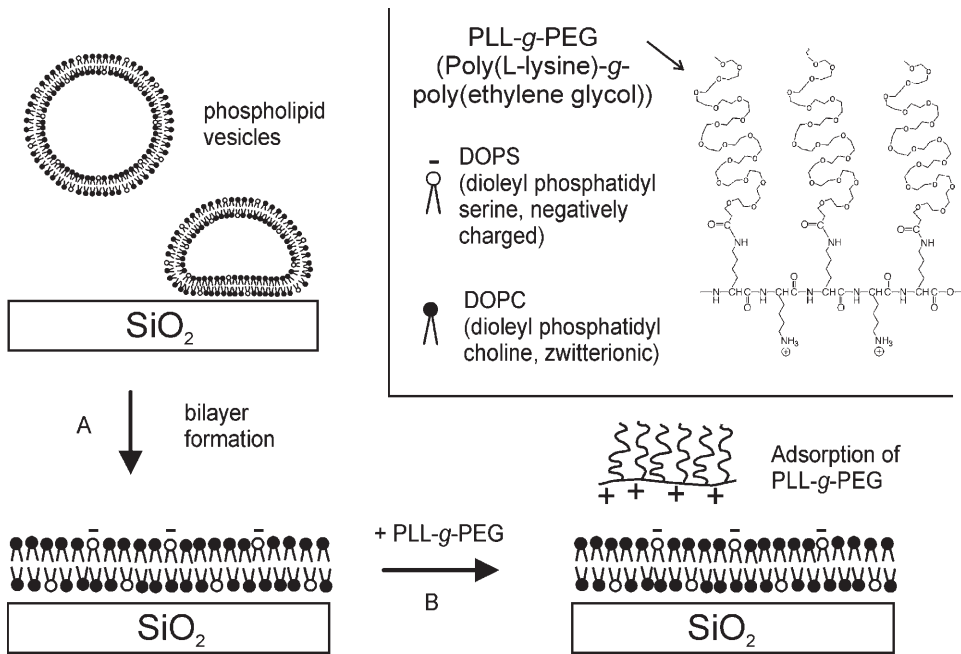
FIGURE 1 Schematic representation of the experimental procedure. (*A*) A supported phospholipid bilayer is formed on a SiO$_2$ surface by vesicle fusion in Ca^{2+} buffer. A bilayer composed of a DOPC (*black head-groups*): DOPS (*white headgroups, negatively charged*) mixture is used in this example; some experiments were performed with SPBs composed of DOPC alone. (*B*) After rinsing with the appropriate buffer(s), PLL-*g*-PEG is added and the interaction with the bilayer is monitored by QCM-D and fluorescence microscopy. The chemical structure of PLL-*g*-PEG and the types of lipids used are shown in the inset.

evaluated in separate experiments with multiple back-and-forth rinses with various buffers.

After the polymer adsorption was considered complete (as judged by the attainment of a stable signal), the excess PLL-*g*-PEG was removed by rinsing with the polymer-free buffer (see Fig. 2 for typical curves). This was followed by a rinse with the Ca^{2+}-containing buffer with which the original baseline was obtained. In this way, the changes in frequency and dissipation factors characteristic of the following stages could be recorded:

1. Bilayer formation: [*frequency of crystal + bilayer*] − [*frequency of the bare crystal*], both in Ca^{2+} buffer.

2. Polymer adsorption on the SPB: [*frequency of crystal + bilayer + polymer*] − [*frequency of crystal + bilayer*], both in the same polymer-free buffer in which the polymer was dissolved.

3. Bilayer with the polymer: [*frequency of crystal + bilayer + polymer*] − [*frequency of the bare crystal*], both in Ca^{2+} buffer.

QCM-D data (frequencies and dissipation factors recorded as a function of time) was imported into a spreadsheet program. The frequency and dissipation factor shifts were calculated by averaging the absolute values of the frequency and dissipation factor over ~10 min periods during which the signals were stable, and subtracting the appropriate average values from
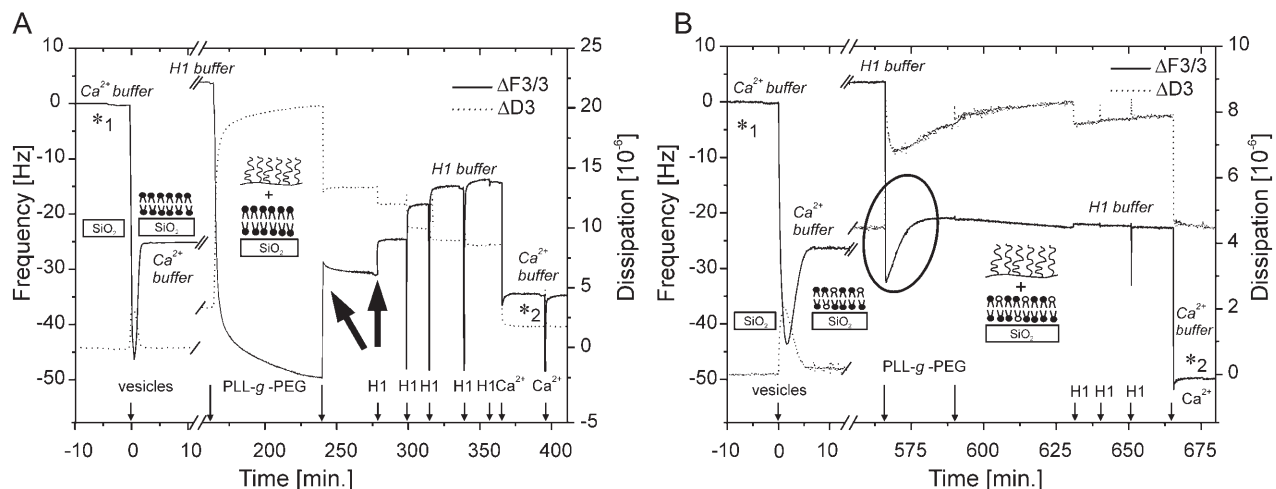

FIGURE 2 Addition of PLL-*g*-PEG in H1 buffer to zwitterionic (*A*) and negatively charged (*B*) bilayers. Arrows along the time axes indicate injections. The various stages of the experiment are indicated with schematic drawings where possible. (*A*) Zwitterionic bilayer (DOPC). Frequency decreases and dissipation factor increases upon addition of PLL-*g*-PEG, indicating copolymer adsorption. However, material is removed from the surface upon both further addition of the polymer and rinsing with H1 buffer (*thick arrows*). (*B*) Negatively charged bilayer (DOPC:DOPS 95:5). Initial adsorption of PLL-*g*-PEG is followed by a spontaneous desorption of material (*encircled*). For clarity and space reasons, some of the buffer exchange steps have been omitted. *1 and *2 indicate the start and endpoints used to calculate the frequency and dissipation shifts shown in Table 1.

one another to obtain the shifts corresponding to situations *1*, *2*, and *3*, above. For convenience, all shifts were scaled by the overtone order.

Fluorescence microscopy

Either an NBD- or a TRITC-labeled phospholipid (NBD-PC and TRITC-PE) or fluorescein-labeled PLL-*g*-PEG was used as the fluorescent species for the experiments performed with a Zeiss LSM 510 confocal laser scanning microscope (Carl Zeiss, Oberkochen, Germany) equipped with a 25-mW Argon laser (lines used: 488 nm and 514 nm).

To prepare SPBs for the observation in the fluorescent microscope, clean SiO$_2$-coated glass slides or QCM-D crystals were incubated with vesicles suspended in Ca^{2+} buffer at 0.5 mg/ml lipid concentration for ~20 min in a right-side-up configuration (protocol *A*) or upside-down configuration (protocol *B*; Cremer and Boxer, 1999, and McConnell et al., 1986). The SPBs were then rinsed to remove excess vesicles—by exchanging the solution above the surface for the Ca^{2+} buffer in the case of protocol *A* or by exposing the surface to a large excess of ultrapure water under stirring in the case of protocol *B*. The water was exchanged for H1 buffer before observation in the fluorescence microscope.

SPBs formed in the chamber of the QCM-D instrument were also examined by fluorescence microscopy. This was done by preparing a fluorescently labeled SPB as described in the previous subsection, unmounting the SPB-coated crystal from the QCM-D instrument, and transferring it to the confocal microscope for analysis. The SPB was never exposed to air during the transfer.

Observation typically began with bleaching a spot on the supported bilayer at full laser power. Recovery of fluorescence was taken to be indicative of bilayer formation (McConnell et al., 1986). Diffusion coefficients (1–2 $\times$ 10^{-8} cm^2/s) and mobile fractions (80–100%) of phospholipids determined from the recovery curves (according to Berquand et al., 2003; and based on the theory published by Axelrod et al., 1976 and Soumpasis, 1983) were found to be in good agreement with literature values for NBD-PE (Wagner and Tamm, 2001; Berquand et al., 2003), NBD-PC, and NBD-PS (Saurel et al., 1998; Cézanne et al., 1999). No changes in the diffusion coefficients or mobile fraction of the probes upon addition of PLL-*g*-PEG were observed.

The SPB was then rinsed with the buffer in which the adsorption of the polymer would be carried out and incubated for 30 min with a solution of polymer dissolved in the appropriate buffer at a concentration of 0.5 mg/ml. Images were recorded at 2-min intervals during this time. The size of the images was 92.1 μm $\times$ 92.1 μm with a pixel size of 0.09 μm $\times$ 0.09 μm. Care was taken to avoid contact of the supported bilayer with air and/or bubbles throughout the experiment to prevent damage to the bilayer.

Supported vesicular layers, or SVLs, were prepared by addition of vesicles to a surface coated with a layer of titanium oxide, prepared and cleaned in the same fashion as the silicon oxide surfaces described above. See Reimhult et al. (2002, 2003) and I. Reviakine, F. F. Rossetti, A. N. Morozov, and M. Textor (unpublished) for detailed discussion of SVL formation and properties.

RESULTS

Interaction of PLL-*g*-PEG with supported bilayers investigated by QCM-D: effects of ionic strength and bilayer composition

QCM-D (Rodahl et al., 1995) is a powerful technique for investigating the formation of thin films on solid surfaces in liquid. It has been used to monitor the formation of supported phospholipid bilayers (SPBs; see Keller and Kasemo, 1998; Reimhult et al., 2003; Richter et al., 2003; Seantier et al., 2004), their protein resistance (Glasmästar et al., 2002), and

other similar processes (Larsson et al., 2003). This technique was therefore used to follow in situ, and in real-time, the interactions between the polyelectrolyte PLL-*g*-PEG and the supported phospholipid bilayers.

PLL-*g*-PEG adsorption in a low ionic strength buffer (H1 buffer)

Typical QCM-D curves obtained when PLL-*g*-PEG was added to zwitterionic and negatively charged bilayers in H1 buffer are shown in Fig. 2, *A* and *B*, respectively. In these experiments, an SPB was first formed from a vesicle suspension in the Ca^{2+} buffer, which was needed for SPB formation from negatively charged vesicles. The buffer was exchanged for the H1 buffer to maximize electrostatic interactions between the SPB and the polyelectrolyte. In separate QCM-D experiments (results not shown) it was found that changing buffers did not significantly perturb the SPBs.

Addition of the PLL-*g*-PEG solution to an SPB in the H1 buffer caused transient changes in the frequency and dissipation shifts consistent with polymer adsorption (Fig. 2). In the case of negatively charged SPBs (Fig. 2 *B*), this adsorption was followed by desorption. In the case of zwitterionic SPBs, further injections of the polymer or rinses were required to initiate the desorption process (see *arrow* in Fig. 2 *A*), indicating that the desorption process was not spontaneous, at least on the timescale of the experiments (typically 60 min).

The total frequency shifts for the SiO$_2$/zwitterionic bilayer/polymer experiments were similar to those observed in the case of polymer adsorbed directly on SiO$_2$ (Tables 1 and 2). In the case of the negatively charged SPBs, significantly larger frequency shifts were observed when the polymer was added to the SPBs than to the bare SiO$_2$ surface. On the other hand, the ΔD values for the SiO$_2$/zwitterionic bilayer/PLL-*g*-PEG experiments performed in H1 buffer were higher than those for PLL-*g*-PEG on bare SiO$_2$ in the same buffer, and increased with the proportion of the negatively charged lipids in the SPB (Tables 1 and 2). The dissipation factor is related to the viscoelastic properties of the layer and its thickness (Voinova et al., 1999). Therefore upon addition of PLL-*g*-PEG the surface layer is converted from an SPB to a thicker and/or less compact layer than either an SPB (Table 1) or a polymer film alone (Table 2). Combined with the observation of the desorption processes (see above), these results suggest that partial replacement of the SPB by PLL-*g*-PEG takes place at the surface. Results of fluorescence microscopy presented below provide further insight into the nature of this process.

No interaction between 2 kDa PEG and the SPBs could be detected by QCM-D.

High ionic strength buffer (EDTA buffer)

In the case of a high ionic strength, Ca^{2+}-free buffer, a small initial adsorption of the copolymer was followed by its

TABLE 1   Total frequency (in Hz) and dissipation shifts ($\times 10^{-6}$, in arbitrary units) for the third overtone observed in the QCM-D experiments with PLL-*g*-PEG in high (EDTA) and low (H1) ionic strength buffers and on supported bilayers of various compositions

	Amount of DOPS (mass %)			
	0%	5%	10%	20%
H1 buffer				
$\Delta F3/3$	-33 ± 2	-41 ± 12	-45	—
$\Delta D3$	1.8 ± 0.1	3.1 ± 2	4.3	—
EDTA buffer				
$\Delta F3/3$	-28 ± 5	—	-29	-26
$\Delta D3$	2.3 ± 2.2	—	-1.2	0.59

The differences between the frequency of the bare crystal in buffer and the frequency of the crystal after the final rinse with the same buffer are reported. They characterize the total amount and properties of material adsorbed on the substrate at the end of the experiment. The frequency and dissipation shifts for the formation of supported bilayers in Ca^{2+} buffer were, independently of composition, $\Delta F3/3 = -26 \pm 1$ and $\Delta D3 = 0.12 \pm 0.4$, respectively. Values with errors are averages of a minimum of three experiments; errors are standard deviations. Values without the standard deviations are single measurements.

partial removal during rinses with the polymer-free buffer. The overall frequency shifts, after the rinses with the Ca^{2+} buffer (for comparison with the initial baseline values acquired in the Ca^{2+} buffer), were larger than those characterizing the bare SPB alone or polymer alone. The overall dissipation shifts were similar to those of the polymer (Tables 1 and 2). This indicates that some polymer did adsorb to the bilayer without displacing the latter.

Interaction of PLL-*g*-PEG with supported bilayers examined by fluorescence microscopy: effect of bilayer quality and composition

To gain further insight into the PLL-*g*-PEG–bilayer interactions, the process was studied by fluorescence microscopy. Depending on the experimental conditions (method by which the bilayer was initially prepared, size of the vesicles used in the preparation, bilayer composition, and buffer ionic strength), different responses to the polymer were observed: they ranged from no changes to the bilayer to complete disruption and removal of the latter from the surface (Table 3).

TABLE 2   Mean values of frequency and dissipation shifts for the adsorption of PLL-*g*-PEG to bare SiO$_2$ crystals in high (EDTA) and low (H1) ionic strength buffers

Buffer	Frequency (Hz)		Dissipation factor (1×10^{-6})	
H1	$\Delta F3/3$	-35 ± 3	$\Delta D3$	1.0 ± 0.7
EDTA buffer	$\Delta F3/3$	-26 ± 4	$\Delta D3$	1.9 ± 0.1

The averages were calculated from a minimum of three experiments and are listed along with the corresponding standard deviations.

High ionic strength buffer (EDTA buffer)

When PLL-*g*-PEG was added to supported bilayers in a high ionic strength buffer, the SPBs were always observed to remain intact, and the copolymer was observed to adsorb to the SPBs (Fig. 3). This response was independent of the quality of the bilayers and of their composition (zwitterionic or negatively charged). These results are consistent with the QCM-D observations.

Low ionic strength buffer (H1 buffer)

Effect of bilayer quality. Exposure of bilayers prepared with protocol *A* from 400-nm vesicles, bilayers exhibiting defects (in the form of holes, attached vesicles, or aggregates), or bilayers damaged by contact with air, to PLL-*g*-PEG in H1 buffer, led to their decomposition (Fig. 4). In the first few seconds to 10 min after addition of PLL-*g*-PEG, small fragments of the bilayer were observed to come off the surface (Fig. 4, *B* and *F*). These fragments assembled spontaneously into globular and worm-like structures (aspect ratio >10; <0.5 μm in diameter and several μm-long, Fig. 4 *D*). Some of the structures were observed to float in solution, whereas others remained anchored to the surface. The removal of the SPB from the surface continued for another ~10 min (Fig. 4, *C* and *G*), but was never complete: some of the lipid remained at the surface after the disruption, most likely in a complex with the adsorbed polymer (not shown). This latter observation is consistent with QCM-D results (see above).

Approximately 30 min after addition of PLL-*g*-PEG, the elongated structures started to collapse into globular structures (Fig. 4 *D*). Using fluorescently labeled PLL-*g*-PEG and TRITC-labeled lipids, it was ascertained that the worm-like structures consisted of polymer-lipid complexes (Fig. 4 *H*), and that both polymer and the lipids were present at the surface after the disruption (not shown). This latter observation is also consistent with QCM-D results (see above).

Using 50-nm vesicles instead of 400-nm ones, adsorbing them on the substrate in an upside-down configuration, and using an enhanced washing procedure (following protocol *B*; Cremer and Boxer, 1999; McConnell et al., 1986), allowed both zwitterionic and negatively charged SPBs that were partially or completely resistant to PLL-*g*-PEG to be prepared (Table 3). Although a significant proportion of the bilayers was still disrupted, these experiments indicate that defects in the SPBs play a role in the disruption process.

SPBs containing fluorescent lipids formed on QCM-D crystals were invariably disrupted upon addition of PLL-*g*-PEG in H1 buffer. This is consistent with the QCM-D results obtained in H1 buffer (Fig. 2).

Effect of polymer architecture. Independent of their quality, both zwitterionic and negatively charged SPBs remained intact after the addition of PLL (20 kDa; see Table 3). Moreover, PLL was found to protect SPBs from subsequent disruption by PLL-*g*-PEG. We infer from this

TABLE 3   Resistance of SPBs formed on SiO$_2$-coated coverslips to disruption by PLL-*g*-PEG in H1 buffer

Bilayer composition	Protocol *A*		Protocol *B*	
DOPC	400-nm vesicles, resistant and partially resistant	43%	50-nm vesicles, resistant and partially resistant	89%
	400-nm vesicles, disrupted	57%	50-nm vesicles, disrupted	11%
DOPC:DOPS 9:1	400-nm, resistant and partially resistant	29%		
	50-nm vesicles, resistant and partially resistant	43%	50-nm vesicles, resistant and partially resistant	50%
	400-nm, disrupted	71%		
	50-nm vesicles, disrupted	57%	50-nm vesicles, disrupted	50%

Samples were classified into three categories according to the degree of disruption of the bilayer 15 min after addition of PLL-*g*-PEG: resistant (appearance identical to that of the bare SPB, Fig. 4 *A, E*), partially resistant (some defects and few wormlike structures present, not shown), and nonresistant (Fig. 4 *C, G*). For this table, the percentages of occurrence of resistant and partially resistant samples were added.

observation that PLL adsorbs to SPBs in H1 buffer—this is, in fact, consistent with previously published observations (Mueller et al., 2000). Therefore, PLL-*g*-PEG is also expected to coat resistant bilayers (see above). The incidence of resistant bilayers in H1 buffer was, however, not sufficiently high to directly test this assertion.

The effect of PEG chain density on the ability of the copolymer to disrupt the bilayer was further investigated by using a copolymer with a high grafting ratio, i.e., low density of PEG chains: PLL(20 kDa)-[*g* = 14.2]-PEG(1 kDa) (Pasche et al., 2003). Both zwitterionic and negatively charged bilayers were found to be resistant to disruption by this copolymer.

No effect of addition of 2-kDa PEG to SPBs could be detected by fluorescence. PEG was also not able to protect the SPBs from subsequent disruption by PLL-*g*-PEG. This is consistent with the observation by QCM-D that PEG does not interact with the SPBs.

Interaction of PLL-*g*-PEG with supported vesicular layers

The effect of PLL-*g*-PEG on supported vesicular layers prepared under the same conditions as the SPBs but on titanium dioxide (adsorption in Ca^{2+} buffer followed by buffer exchange to H1 before polymer addition) was investigated by fluorescence microscopy (Fig. 4, *I–L*). It was found that neither the zwitterionic nor the negatively charged vesicles were decomposed by the polymer, and no formation of worms was observed. However, the zwitterionic vesicles were displaced from the substrate by PLL-*g*-PEG, whereas the negatively charged ones were not.

DISCUSSION

The disruption of supported bilayers by PLL-*g*-PEG in a low-ionic strength buffer is an interesting phenomenon. Given that under identical conditions, the copolymer does not induce decomposition of surface-adsorbed vesicles (Fig. 4, *I–L*), it illustrates the limitations of supported bilayers as a model system for free-standing lipidic structures such as cell membranes and vesicle walls. In what follows, the mechanism of this disruption is considered in terms of the influence of polymer architecture, bilayer quality (presence or absence of defects), and the solid support, on the disruption process.

Interactions between charged vesicles and polyelectrolytes, including poly(lysine), have been studied in detail. In particular, adsorption of poly(*n*-ethyl-4-vinylpyridinium bromide) to vesicles containing cardiolipin (CL) resulted in the transfer of the latter to the outer leaflet of the membrane due to the enhancement of the flip-flop rate. Vesicles containing >20–30% CL were ultimately destroyed by the polymer (Yaroslavov et al., 1998). Pure CL liposomes were found to undergo a transformation to multilamellar lipid-polymer complexes upon addition of PLL (de Kruijff et al., 1985). High molecular weight PLL was also found to destabilize black lipid membranes composed of pure PS (Diederich et al., 1998).
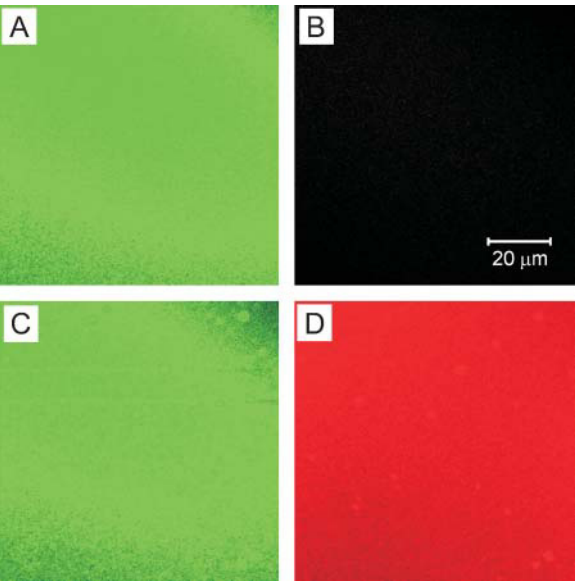
FIGURE 3   Fluorescence signals arising from a DOPC:DOPS 9:1 bilayer doped with TRITC-PE (*green*) and from PLL-*g*-PEG-fluorescein (*red*) for an SPB alone (*A, B*) and for an SPB coated with PLL-*g*-PEG in EDTA buffer after rinsing away the excess polymer (*C, D*). The images were taken under identical conditions using the laser lines appropriate for each probe, and demonstrate that after the addition of PLL-*g*-PEG-fluorescein, the previously bare SPB (*A, B*) remains intact (*C*) and is coated with the polymer (*D*).
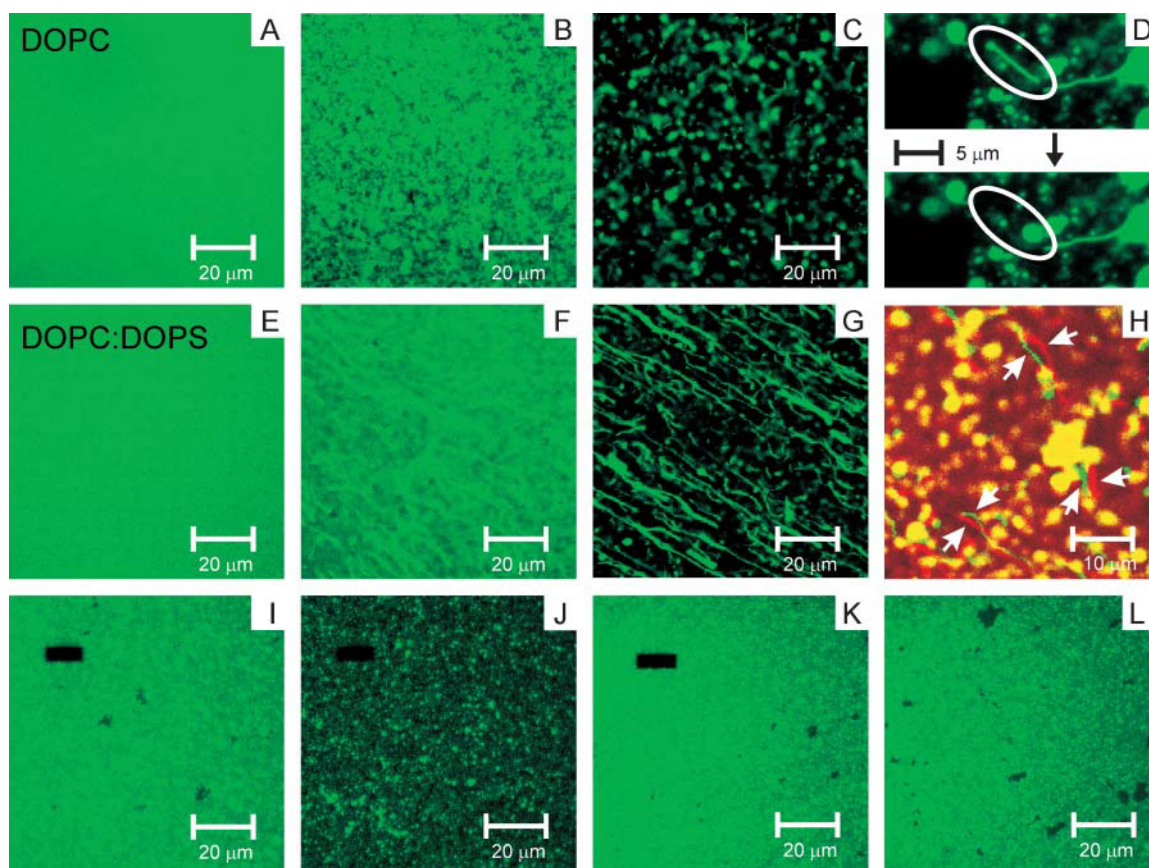
FIGURE 4 Time-lapse sequences of false-colored fluorescence images depicting the disruption of supported bilayers on SiO$_2$ (*A–H*) and the interaction of PLL-*g*-PEG in H1 with supported vesicular layers on TiO$_2$ (*I–L*). The green color corresponds to the lipids. (*A–C*) A DOPC bilayer, doped with 1% NBD-PC, before (*A*), a few seconds after (*B*), and 30 min after (*C*) the addition of PLL-*g*-PEG in H1 buffer. (*D*) The worms formed during the bilayer disruption were observed to collapse into globular structures (*encircled*). Two sequential images taken 45 min after PLL-*g*-PEG addition, 60 s apart, are shown. The collapse is instantaneous. (*E–G*) A DOPC:DOPS 9:1 bilayer, doped with 1% NBD-PC, before (*E*), 1 min after (*F*), and 5 min after (*G*) PLL-*g*-PEG addition in H1 buffer. (*H*) A fluorescence image demonstrating the colocalization of phospholipids (*green*) and PLL-*g*-PEG-fluorescein (*red*) in the worm-like structures and aggregates that form after the disruption of a of DOPC:DOPS 9:1 SPB. The polymer was added in H1 buffer. Some worms appear as double lines (one in *green* and one in *red*) in the images (*white arrowheads*) due to their movement during the time passed between the acquisition of the images in the two channels. Colocalization was also observed in the case of DOPC bilayers (not shown). (*I–J*) Zwitterionic (DOPC) vesicles adsorbed on the surface of TiO$_2$ form a supported vesicular layer (*I*). They are replaced on the surface by the adsorbing PLL-g-PEG (*J*). (*K–L*) The copolymer has no effect on the negatively charged (DOPC:DOPS 9:1) vesicles. The average intensity of the images is the same before (*K*) and after (*L*) the addition of the polymer. In both cases, the vesicles remain intact. Formation of wormlike structures is not observed. Vesicles were labeled with NBD-PC.

In the case of bilayers with lower charge density (such as those used in this study), polycations have been found to adsorb to the vesicle surface without disrupting the latter, but only perturbing the packing of the lipids in the membrane (Huster et al., 2000), causing a shift in the gel-to-liquid transition temperature (Chapman et al., 1974; Carrier and Pézolet, 1986), and causing domain formation for stoichiometric ratios of polymer to lipid smaller than one (Franzin and Macdonald, 2001). Thus, disruption of the SPBs by a polyelectrolyte is not expected under the experimental conditions employed in this study (typically 10% of DOPS and excess of PLL or PLL-*g*-PEG), and neither is domain formation (which could lead to formation of defects in the SPB). Indeed, PLL by itself was not found to cause the disruption of the SPBs (Table 3). Compared to PLL, PLL-*g*-PEG with a grafting ratio of ~3 has an ~30% smaller charge density (only the fraction 1–1/*g* of the amino groups of PLL remains free, whereas the rest are involved in the amide linkage to the PEG side chains and are uncharged). Therefore, PLL-*g*-PEG-induced disruption of bilayers in a low ionic strength buffer (Fig. 4) does not proceed by a mechanism typical of polyelectrolytes, such as those observed in the studies mentioned above. It is instead related to the copolymer architecture. Upon adsorption of the copolymer to a flat surface, such as that of an oxide or an SPB, the volume available to the PEG chains is significantly reduced compared to that available to them in solution. In the case when the distance between the grafting points along the PLL backbone, *L*, is smaller than the radius of gyration of the PEG chains, R_{gPEG} (Kawaguchi et al., 1997)—in other words, when L/R_{gPEG} is smaller than one—the PEG chains are laterally compressed upon adsorption (de Gennes, 1987).

Simple calculation (taking the lysine monomer length at ~0.355 nm based on the distance between the α-carbon atoms in a typical β-sheet structure, R_g of 2 kDa PEG at 1.7 nm, and R_g of 1 kDa PEG at 1.1 nm; Kawaguchi et al., 1997) shows that in the case of PLL(20)-g2.9-PEG(2), which disrupts the bilayers, this ratio is ~0.4, whereas in the case of PLL(20)-g14.2-PEG(1), which does not, the ratio is ~4.5. Compression of PEG chains incurs an entropic penalty. The chains can expand, and the free energy of the system can be lowered, if the PLL backbone is allowed to curve. This induces curvature in the underlying bilayer to which the copolymer is bound, and thus lifts the bilayer off the surface (Fig. 5). Natural curvature of the membrane in liposomes may therefore constitute one reason why they are resistant to decomposition by PLL-g-PEG (preliminary studies have also indicated that PLL-g-PEG does not induce leakage in 50-nm-diameter liposomes; not shown). Other reasons may include the fact that a portion of the surface area of the liposomes is stored as membrane fluctuations (see Seifert, 1997), and that these fluctuations are damped by the presence of the solid support (see Podgornik and Parsegian, 1992) and the ability of the liposomes to change shape.

Better-quality bilayers (it has been reported by several investigators that the use of smaller—i.e., 50 nm instead of 400 nm—vesicles leads to better quality bilayers and improves reproducibility of experiments with SPBs; see Cremer and Boxer, 1999; Reimhult et al., 2002) were less likely to be disrupted by PLL-g-PEG (Table 3). Exposure of the bilayers to air invariably led to their destruction by the copolymer. These observations suggest that defects play a crucial role in the disruption process. This is once again consistent with the observation that liposomes, which essentially lack defects if prepared from fluid-phase lipids, are resistant to decomposition by the copolymer (Fig. 4, I–L).
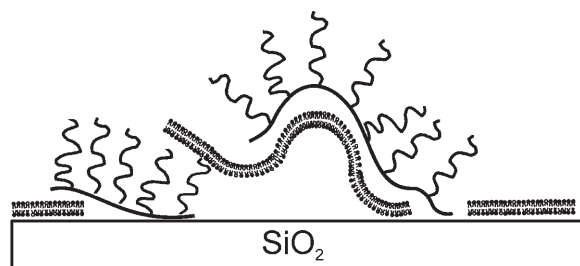

FIGURE 5 Interpretation of the bilayer disruption mechanism. Upon adsorption of the copolymer to a flat surface of an SPB, the PEG chains are compressed. This process is entropically costly, and the free energy of the system is lowered by bending the bilayer and lifting it off of the underlying substrate. The process involves bilayer rupture and is therefore thought to nucleate at pre-existing defects or be facilitated by osmotic and electrical gradients that destabilize the bilayer. When the disruption process is completed, most of the lipids are floating in solution in the form of worm-like lipid-PLL-g-PEG complexes. The copolymer also coats the SiO$_2$ substrate with the remains of bilayer.

The role of defects in the disruption process can be understood if one considers that destruction of the bilayer by any mechanism, including the one outlined above (Fig. 5), must invariably proceed via bilayer rupture. This is a thermally activated process (Shillcock and Seifert, 1998). A pre-existing defect will therefore serve as an efficient nucleation center for the disruption by lowering the activation energy required for the disruption process to commence. As to the source of the defects, some authors have argued that preparing a defect-free SPB by a vesicle fusion procedure is virtually impossible (Rädler et al., 1995; Sackmann, 1996; Steinem et al., 1996; Wiegand et al., 2002). Furthermore, buffer exchange, inherent in the experimental procedure used here, may also have contributed to the formation of defects in the SPB that are below the detection limit of the QCM-D as well as to the destabilization of the SPB in general: Diederich et al. (1998) have observed that black lipid membranes were more sensitive to destabilization by PLL in the presence of only 10 mM salt than in the presence of 100 mM salt. Additionally, the exchange of buffers on one side of the bilayer only, may induce osmotic and electrical gradients across the bilayer.

It is interesting to note that SPBs prepared on QCM-D crystals were invariably disrupted by PLL-g-PEG added in H1 buffer, suggesting that their quality was not as good as of those prepared on silicon oxide-coated glass slides. Yet it has previously been shown that SPBs prepared on QCM-D crystals are quite effective in preventing nonspecific adsorption of proteins to surfaces they cover (Glasmästar et al., 2002). The contradiction between this finding and our result is only apparent, however, because to initiate the disruption process, the defects need not be either large or numerous (Diederich et al., 1998)—they can be quite small (pinholes); too small for the proteins to adsorb or for the adsorption of a small amount of proteins to be detected. Furthermore, nonspecific protein adsorption to the defects in the bilayer is a self-limiting process (no more protein adsorbs once the defects are filled), whereas the decomposition by PLL-g-PEG is autocatalytic (removal of a portion of the bilayer creates a nucleation point for further removal).

The stability of the bilayers to disruption by PLL-g-PEG in a high ionic strength buffer (EDTA buffer) can be explained in terms of improved overall bilayer stability in the presence of salt, different conformation of the polymer backbone at a high ionic strength, smaller amount of polymer adsorbed to the surface, or a combination of these factors. Currently it is not possible to differentiate between them. The fact that the copolymer was observed to interact with the bilayers at high ionic strength at all (Fig. 3) is consistent with the previously published accounts of polymer adsorption to liposomes in the presence of electrolytes (Franzin and Macdonald, 2001). There is some controversy in the literature with respect to the binding of ionic polymers to bilayers composed of zwitterionic lipids, such as dimyristoyl phosphatidyl choline (see Laroche et al., 1988). Here we

clearly observed disruption of DOPC SPBs by PLL-*g*-PEG in a low ionic strength buffer (Fig. 4, *A–D*) and some adsorption in a high-ionic strength one. This phenomenon has likely the same cause as the adsorption of divalent cations to DOPC bilayers (Lis et al., 1981; Huster and Arnold, 1998).

CONCLUSIONS

We have shown that the graft copolymer PLL-*g*-PEG disrupts supported phospholipid bilayers in a low ionic strength buffer, but not in a high ionic strength one. Copolymer architecture was found to play a significant role in the bilayer disruption. This is attributed to the entropic cost associated with compressing the PEG side chains of the copolymer when it adsorbs to a planar surface of an SPB. The free energy of the system is lowered by inducing curvature in the underlying bilayer, which leads to the removal of the latter from the surface. This process appears to be initiated at the defects present in the SPBs, thus preparation methods that improve the quality of SPBs led to higher incidence of bilayers resistant to disruption by PLL-*g*-PEG even in low ionic strength buffers. Surface-bound phospholipid vesicles were not decomposed by PLL-*g*-PEG under the same conditions. This observation supports the proposed disruption mechanism and illustrates the significance of the subtle differences between the two systems (supported bilayers and vesicles).

REFERENCES

Alberts, B., D. Bray, J. Lewis, M. Raff, K. Roberts, and J. D. Watson. 1994. Molecular Biology of the Cell. Garland Publishing, New York.

Axelrod, D., D. E. Koppel, J. Schlessinger, E. Elson, and W. W. Webb. 1976. Mobility measurement by analysis of fluorescence photobleaching recovery kinetics. *Biophys. J.* 16:1055–1069.

Berquand, A., P.-E. Mazeran, J. Pantigny, V. Proux-Delrouyre, J.-M. Laval, and C. Bourdillon. 2003. Two-step formation of streptavidin-supported lipid bilayers by PEG-triggered vesicle fusion. Fluorescence and atomic force microscopy characterization. *Langmuir.* 19:1700–1707.

Bronich, T. K., S. V. Solomatin, A. A. Yaroslavov, A. Eisenberg, V. A. Kabanov, and A. V. Kabanov. 2000. Steric stabilization of negatively charged liposomes by cationic graft copolymer. *Langmuir.* 16:4877–4881.

Carrier, D., and M. Pézolet. 1986. Investigation of polylysine-dipalmitoyl-phosphatidylglycerol interactions in model membranes. *Biochemistry.* 25:4167–4174.

Cézanne, L., A. Lopez, F. Loste, G. Parnaud, O. Saurel, P. Demange, and J.-F. Tocanne. 1999. Organization and dynamics of the proteolipid complexes formed by annexin V and lipids in planar supported lipid bilayers. *Biochemistry.* 38:2779–2786.

Chapman, D., J. Urbina, and K. M. Keough. 1974. Biomembrane phase transitions. Studies of lipid-water systems using differential scanning calorimetry. *J. Biol. Chem.* 249:2512–2521.

Cremer, P. S., and S. G. Boxer. 1999. Formation and spreading of lipid bilayers on planar glass supports. *J. Phys. Chem. B.* 103:2554–2559.

Csúcs, G., R. Michel, J. W. Lussi, M. Textor, and G. Danuser. 2003. Microcontact printing of novel co-polymers in combination with proteins for cell-biological applications. *Biomaterials.* 24:1713–1720.

de Gennes, P. G. 1987. Polymers at an interface: a simplified view. *Adv. Colloid Interface Sci.* 27:189–209.

de Kruijff, B., A. Rietveld, N. Telders, and B. Vaandrager. 1985. Molecular aspects of the bilayer stabilization induced by poly(L-lysines) of varying size in cardiolipin liposomes. *Biochim. Biophys. Acta.* 820:295–304.

Diederich, A., G. Bahr, and M. Winterhalter. 1998. Influence of polylysine on the rupture of negatively charged membranes. *Langmuir.* 14:4597–4605.

Elbert, D. L., and J. A. Hubbell. 1998. Self-assembly and steric stabilization at heterogeneous, biological surfaces using adsorbing block copolymers. *Chem. Biol.* 5:177–183.

Epand, R. M. 2003. Fusion peptides and the mechanism of viral fusion. *Biochim. Biophys. Acta.* 1614:116–121.

Franzin, C. M., and P. M. Macdonald. 2001. Polylysine-induced ^{2}H NMR-observable domains in phosphatidylserine/phosphatidylcholine lipid bilayers. *Biophys. J.* 81:3346–3362.

Ge, L., H. Möhwald, and J. Li. 2003. Polymer-stabilized phospholipid vesicles formed on polyelectrolyte multilayer capsules. *Biochem. Biophys. Res. Commun.* 303:653–659.

Glasmästar, K., C. Larsson, F. Höök, and B. Kasemo. 2002. Protein adsorption on supported phospholipid bilayers. *J. Colloid Interface Sci.* 246:40–47.

Golubovic, L., and M. Golubovic. 1998. Fluctuations of quasi-two-dimensional smectics intercalated between membranes in multilamellar phases of DNA cationic lipid complexes. *Phys. Rev. Lett.* 80:4341–4344.

Hartmann, W., and H. J. Galla. 1978. Binding of polylysine to charged bilayer membranes—molecular organization of a lipid-peptide complex. *Biochim. Biophys. Acta.* 509:474–490.

Heimburg, T., B. Angerstein, and D. Marsh. 1999. Binding of peripheral proteins to mixed lipid membranes: effect of lipid demixing upon binding. *Biophys. J.* 76:2575–2586.

Heimburg, T., and D. Marsh. 1995. Protein surface-distribution and protein-protein interactions in the binding of peripheral proteins to charged lipid membranes. *Biophys. J.* 68:536–546.

Huang, N.-P., R. Michel, J. Vörös, M. Textor, R. Hofer, A. Rossi, D. L. Elbert, J. A. Hubbell, and N. D. Spencer. 2001. Poly(L-lysine)-*g*-poly(ethylene glycol) layers on metal oxide surfaces: surface-analytical characterization and resistance to serum and fibrinogen adsorption. *Langmuir.* 17:489–498.

Huang, N.-P., J. Vörös, S. M. De Paul, M. Textor, and N. D. Spencer. 2002. Biotin-derivatized poly(L-lysine)-*g*-poly(ethylene glycol): a novel polymeric interface for bioaffinity sensing. *Langmuir.* 18:220–230.

Huster, D., and K. Arnold. 1998. Ca^{2+}-mediated interaction between dextran sulfate and dimyristoyl-*sn*-glycero-3-phosphocholine surfaces studied by ^{2}H nuclear magnetic resonance. *Biophys. J.* 75:909–916.

Huster, D., U. Dietrich, T. Gutberlet, K. Gawrisch, and K. Arnold. 2000. Lipid matrix properties in cationic membranes interacting with anionic polyelectrolytes: a solid-state NMR approach. *Langmuir.* 16:9225–9232.

Kawaguchi, S., G. Imai, J. Suzuki, A. Miyahara, and T. Kitano. 1997. Aqueous solution properties of oligo- and poly(ethylene oxide) by static light scattering and intrinsic viscosity. *Polymer.* 38:2885–2891.

Kawakami, K., Y. Nishihara, and K. Hirano. 2001. Effect of hydrophilic polymers on physical stability of liposome dispersions. *J. Phys. Chem. B.* 105:2374–2385.

Keller, C. A., and B. Kasemo. 1998. Surface specific kinetics of lipid vesicle adsorption measured with a quartz crystal microbalance. *Biophys. J.* 75:1397–1402.

Kenausis, G. L., J. Vörös, D. L. Elbert, N.-P. Huang, R. Hofer, L. Ruiz-Taylor, M. Textor, J. A. Hubbell, and N. D. Spencer. 2000. Poly(L-lysine)-g-poly(ethylene glycol) layers on metal oxide surfaces: attachment mechanism and effects of polymer architecture on resistance to protein adsorption. *J. Phys. Chem. B.* 104:3298–3309.

Kim, J. Y., M. Mosior, L. A. Chung, H. Wu, and S. McLaughlin. 1991. Binding of peptides with basic residues to membranes containing acidic phospholipids. *Biophys. J.* 60:135–148.

Kleinschmidt, J. H., and D. Marsh. 1997. Spin-label electron spin resonance studies on the interactions of lysine peptides with phospholipid membranes. *Biophys. J.* 73:2546–2555.

Kozlova, N. O., I. B. Bruskovskaya, I. B. Okuneva, N. S. Melik-Nubarov, A. A. Yaroslavov, V. A. Kabanov, and F. M. Menger. 2001. Interaction of a cationic polymer with negatively charged proteoliposomes. *Biochim. Biophys. Acta.* 1514:139–151.

Kuhn, R. J., W. Zhang, M. G. Rossmann, S. V. Pletnev, J. Corver, E. Lenches, C. T. Jones, S. Mukhopadhyay, P. R. Chipman, E. G. Strauss, T. S. Baker, and J. H. Strauss. 2002. Structure of Dengue virus: implications for flavivirus organization, maturation, and fusion. *Cell.* 108:717–725.

Kurrat, R., M. Textor, J. J. Ramsden, P. Böni, and N. D. Spencer. 1997. Instrumental improvements in optical waveguide light mode spectroscopy for the study of biomolecule adsorption. *Rev. Sci. Instrum.* 68:2172–2176.

Ladavière, C., C. Tribet, and S. Cribier. 2002. Lateral organization of lipid membranes induced by amphiphilic polymer inclusions. *Langmuir.* 18:7320–7327.

Laroche, G., D. Carrier, and M. Pezolet. 1988. Study of the effect of poly(L-lysine) on phosphatidic acid and phosphatidylcholine/phosphatidic acid bilayers by Raman spectroscopy. *Biochemistry.* 27:6220–6228.

Larsson, C., M. Rodahl, and F. Höök. 2003. Characterization of DNA immobilization and subsequent hybridization on a 2D arrangement of streptavidin on a biotin-modified lipid bilayer supported on SiO$_2$. *Anal. Chem.* 75:5080–5087.

Lipowsky, R. 1995. Bending of membranes by anchored polymers. *Europhys. Lett.* 30:197–202.

Lis, L. J., V. A. Parsegian, and R. P. Rand. 1981. Binding of divalent cations to dipalmitoylphosphatidylcholine bilayers and its effect on bilayer interaction. *Biochemistry.* 20:1761–1770.

Macdonald, P. M., K. J. Crowell, C. M. Franzin, P. Mitrakos, and D. J. Semchyschyn. 1998. Polyelectrolyte-induced domains in lipid bilayer membranes: the deuterium NMR perspective. *Biochem. Cell Biol.* 76:452–464.

McConnell, H. M., T. H. Watts, R. M. Weis, and A. A. Brian. 1986. Supported planar membranes in studies of cell-cell recognition in the immune system. *Biochim. Biophys. Acta.* 864:95–106.

Mueller, H., H. J. Butt, and E. Bamberg. 2000. Atomic force microscopy deposition of poly-L-lysine structures onto lipid bilayers supported by mica. *Langmuir.* 16:9568–9570.

Nollert, P., H. Kiefer, and F. Jahnig. 1995. Lipid vesicle adsorption versus formation of planar bilayers on solid surfaces. *Biophys. J.* 69:1447–1455.

O'Hern, C. S., and T. C. Lubensky. 1998. Sliding columnar phase of DNA lipid complexes. *Phys. Rev. Lett.* 80:4345–4348.

Pasche, S., S. M. De Paul, J. Vörös, N. D. Spencer, and M. Textor. 2003. Poly(L-lysine)-graft-poly(ethylene glycol) assembled monolayers on niobium oxide surfaces: a quantitative study of the influence of polymer interfacial architecture on resistance to protein adsorption by TOF-SIMS and in situ OWLS. *Langmuir.* 19:9216–9225.

Peisajovich, S. G., and Y. Shai. 2003. Viral fusion proteins: multiple regions contribute to membrane fusion. *Biochim. Biophys. Acta.* 1614:122–129.

Pfohl, T., Y. Li, J. H. Kim, Z. Wen, G. C. L. Wong, I. Koltover, M. W. Kim, and C. R. Safinya. 2002. Biological polyelectrolyte complexes in solution and confined on patterned surfaces. *Colloid Surf. A.* 198–200:613–623.

Podgornik, R., and V. A. Parsegian. 1992. Thermal mechanical fluctuations of fluid membranes in confined geometries—the case of soft confinement. *Langmuir.* 8:557–562.

Rädler, J., H. Strey, and E. Sackmann. 1995. Phenomenology and kinetics of lipid bilayer spreading on hydrophilic surfaces. *Langmuir.* 11:4539–4548.

Reimhult, E., F. Höök, and B. Kasemo. 2002. Vesicle adsorption on SiO$_2$ and TiO$_2$: dependence on vesicle size. *J. Chem. Phys.* 117:7401–7404.

Reimhult, E., F. Höök, and B. Kasemo. 2003. Intact vesicle adsorption and supported biomembrane formation from vesicles in solution: influence of surface chemistry, vesicle size, temperature, and osmotic pressure. *Langmuir.* 19:1681–1691.

Richter, R., A. Mukhopadhyay, and A. Brisson. 2003. Pathways of lipid vesicle deposition on solid surfaces: a combined QCM-D and AFM study. *Biophys. J.* 85:3035–3047.

Ringsdorf, H., E. Sackmann, J. Simon, and F. M. Winnik. 1993. Interactions of liposomes and hydrophobically modified poly-(n-isopropylacrylamides): an attempt to model the cytoskeleton. *Biochim. Biophys. Acta.* 1153:335–344.

Rodahl, M., F. Höök, A. Krozer, P. Brzezinski, and B. Kasemo. 1995. Quartz-crystal microbalance setup for frequency and q-factor measurements in gaseous and liquid environments. *Rev. Sci. Instrum.* 66:3924–3930.

Ruiz-Taylor, L. A., T. L. Martin, and P. Wagner. 2001a. X-ray photoelectron spectroscopy and radiometry studies of biotin-derivatized poly(L-lysine)-grafted-poly(ethylene glycol) monolayers on metal oxides. *Langmuir.* 17:7313–7322.

Ruiz-Taylor, L. A., T. L. Martin, F. G. Zaugg, K. Witte, P. Indermuhle, S. Nock, and P. Wagner. 2001b. Monolayers of derivatized poly(L-lysine)-grafted poly(ethylene glycol) on metal oxides as a class of biomolecular interfaces. *Proc. Nat. Acad. Sci. USA.* 98:852–857.

Sackmann, E. 1996. Supported membranes: scientific and practical applications. *Science.* 271:43–48.

Sackmann, E., and M. Tanaka. 2000. Supported membranes on soft polymer cushions: fabrication, characterization and applications. *Trends Biotechnol.* 18:58–64.

Sagristá, M. L., M. Mora, and M. A. De Madariaga. 2000. Surface modified liposomes by coating with charged hydrophilic molecules. *Cell. Mol. Biol. Lett.* 5:19–33.

Saurel, O., L. Cézanne, A. Milon, J.-F. Tocanne, and P. Demange. 1998. Influence of annexin V on the structure and dynamics of phosphatidylcholine/phosphatidylserine bilayers: a fluorescence and NMR study. *Biochemistry.* 37:1403–1410.

Sawhney, A. S., and J. A. Hubbell. 1992. Poly(ethylene oxide)-graft-poly(L-lysine) copolymers to enhance the biocompatibility of poly(L-lysine)-alginate microcapsule membranes. *Biomaterials.* 13:863–870.

Seantier, B., C. Breffa, O. Félix, and G. Decher. 2004. In situ investigations of the formation of mixed supported lipid bilayers close to the phase transition temperature. *Nano Lett.* 4:5–10.

Seifert, U. 1997. Configurations of fluid membranes and vesicles. *Adv. Phys.* 46:13–137.

Shillcock, J. C., and U. Seifert. 1998. Thermally induced proliferation of pores in a model fluid membrane. *Biophys. J.* 74:1754–1766.

Soumpasis, D. M. 1983. Theoretical-analysis of fluorescence photobleaching recovery experiments. *Biophys. J.* 41:95–97.

Steinem, C., A. Janshoff, W.-P. Ulrich, M. Sieber, and H.-J. Galla. 1996. Impedance analysis of supported lipid bilayer membranes: a scrutiny of different preparation techniques. *Biochim. Biophys. Acta.* 1279:169–180.

Sweitzer, S. M., and J. E. Hinshaw. 1998. Dynamin undergoes a GTP-dependent conformational change causing vesiculation. *Cell.* 93:1021–1029.

Terrettaz, S., M. Mayer, and H. Vogel. 2003. Highly electrically insulating tethered lipid bilayers for probing the function of ion channel proteins. *Langmuir*. 19:5567–5569.

VandeVondele, S., J. Vörös, and J. A. Hubbell. 2003. RGD-grafted poly-L-lysine-graft-(polyethylene glycol) copolymers block non-specific protein adsorption while promoting cell adhesion. *Biotechnol. Bioeng.* 82:784–790.

Voinova, M. V., M. Rodahl, M. Jonson, and B. Kasemo. 1999. Viscoelastic acoustic response of layered polymer films at fluid-solid interfaces: continuum mechanics approach. *Phys. Scripta*. 59:391–396.

Wagner, M. L., and L. K. Tamm. 2001. Reconstituted syntaxin1A/SNAP25 interacts with negatively charged lipids as measured by lateral diffusion in planar supported bilayers. *Biophys. J.* 81:266–275.

Wang, F., G. H. Naisbitt, L. P. Vernon, and M. Glaser. 1993. *Pyrularia* thionin binding to and the role of tryptophan-8 in the enhancement of phosphatidylserine domains in erythrocyte membranes. *Biochemistry*. 32:12283–12289.

Watts, T. H., A. A. Brian, J. W. Kappler, P. Marrack, and H. M. McConnell. 1984. Antigen presentation by supported planar membranes containing affinity-purified I-AD. *Proc. Nat. Acad. Sci. USA*. 81:7564–7568.

Wiegand, G., N. Arribas-Layton, H. Hillebrandt, E. Sackmann, and P. Wagner. 2002. Electrical properties of supported lipid bilayer membranes. *J. Phys. Chem. B*. 106:4245–4254.

Woodle, M. C., and D. D. Lasic. 1992. Sterically stabilized liposomes. *Biochim. Biophys. Acta*. 1113:171–199.

Yaroslavov, A. A., E. A. Kiseliova, O. Y. Udalykh, and V. A. Kabanov. 1998. Integrity of mixed liposomes contacting a polycation depends on the negatively charged lipid content. *Langmuir*. 14:5160–5163.

Yaroslavov, A. A., O. Y. Kuchenkova, I. B. Okuneva, N. S. Melik-Nubarov, N. O. Kozlova, V. I. Lobyshev, F. M. Menger, and V. A. Kabanov. 2003. Effect of polylysine on transformations and permeability of negative vesicular membranes. *Biochim. Biophys. Acta*. 1611:44–54.